

*The Effects of Distortion on Trajectory of Diesel particulate
Matter (PM) from Mobile Sources*

FINAL REPORT

Hamid R. Rahai, Ph.D. and Antonella Sciortino, Ph.D.

Center for Energy and Environmental Research and Services (CEERS)
College of Engineering
California State University Long Beach

CSULB-METRANS contract number 07-361909

April 1, 2012

Disclaimer

The contents of this report reflect the views of the authors, who are responsible for the facts and the accuracy of the information presented herein. This document is disseminated under the sponsorship of the Department of Transportation, University Transportation Centers Program, and California Department of Transportation in the interest of information exchange. The U.S. Government and California Department of Transportation assume no liability for the contents or use thereof. The contents do not necessarily reflect the official views or policies of the State of California or the Department of Transportation. This report does not constitute a standard, specification, or regulation.

Abstract

Laboratory and field measurements were performed to understand the effects of local urban aerodynamics on PM concentration. For the laboratory experiments, an open-circuit wind tunnel along with exhaust from a small diesel engine were used. The ratios of the exhaust mean velocity to the free stream mean velocity were 12.4, 5.7, and 3.9. The blockage models were a rectangular object and a cylinder with nearly the same projected area, spanning the height of the wind tunnel cross section at the mid-section.

The field measurements were performed along the Alameda Corridor railroad at the Commodore Heim Bridge, at the intersection of the Henry Ford and Anchorage roads. The field tests were performed under the bridge adjacent to the control room at the location where distortion due to the building structure was present.

The overall results indicate that the PM concentration is a function of the local wind speed and direction and the blockage effect. Increased wind toward the structures and higher blockage results in increased PM concentration. Based on the laboratory results, an exponential function has been proposed for prediction of the PM concentration with respect to the local mean velocity and distance from obstructions. However, further field tests are recommended for various locations and structures for development of a more generalized model for predicting PM concentration within urban areas.

Table of Contents

DISCLAIMER	2
ABSTRACT	3
TABLE OF CONTENTS	4
LIST OF FIGURES	5
DISCLOSURE	6
ACKNOWLEDGEMENT	7
INTRODUCTION	8
BACKGROUND	9
MEASUREMENT SYSTEMS, PROCEDURE AND TECHNIQUES	10
RESULTS AND DISCUSSIONS	13
CONCLUSIONS	19
REFERENCES	20

LIST OF FIGURES

Figures	Page
1. Flow through an urban area.....	8
2. The open-circuit wind tunnel.....	11
3. Diesel exhaust.....	12
4. The distorting objects.....	12
5. Field test measurements.....	13
6. Variation of the free stream mean velocity and PM concentration for the cylinder.....	13
7. Variation of the free stream mean velocity and PM concentration for the rectangular object.....	14
8. Variation of the normalized mean velocity along the mean stagnation streamlines for (a)2.7 MPH, (b) 5.8MPH, and (c) 8.2 MPH.....	15
9. Variation of normalized PM at free stream velocity of (a) 2.7 MPH, (b) 5.8 MPH, (c) 8.2 MPH.....	15
10. Variation of normalized scalar from equation 2 at free stream velocity of (a) 2.7 MPH, (b) 5.8 MPH, (c) 8.2 MPH.....	16
11. Variation of the ratio of normalized PM to normalized velocity with upstream distance.....	17
12. Temporal variation of PM, wind speed and direction from the field test measurements at $x=h$	18
13. Temporal variation of PM, wind speed and direction from the field test measurements near the wall.....	18

Disclosure

Project was funded in entirety under this contract to California Department of Transportation.

Acknowledgments

This study was supported with a grant from METRANS research program. The authors would like to thank METRANS executive committee for their support. The supports of CSULB graduate assistants, Jeremy Bonifacio and Ehsan Shamloo, CEERS technical support staff, and Mr. Mike Fritz and Mr. Joe Wardell of CSULB Mechanical and Aerospace Engineering technicians, are gratefully acknowledged. The authors would like to thank Dr. Geraldine Knatz, executive director of the port of Los Angeles (LA), Mr. Ron Groves of the Engineering Division of the Port of LA, and Mr. Mike Stolzman of the Pacific Harbor Line (PHL) for their supports during the field tests. The results presented in this report are also part of the M.S. thesis of Mr. Ehsan Shamloo Aliabadi for a Master of Science degree in Engineering with concentration in Environmental Engineering at CSULB.

INTRODUCTION

There are strong evidences that inhaled pollutants can have adverse effects on lung and heart. It is also possible that the inhaled particulates travel into the brain along nerves from nasal passages or/and transported via the blood stream from the lungs. Clinical studies on dogs and mice have shown significant increases in the levels of inflammatory markers and abnormal protein deposits in the brain of animals that are exposed to high level of particulate matter (PM) [1]. These markers and abnormality are also seen in patients' preceding conditions to the onset of the Alzheimer disease. Although further clinical studies and research are needed to assess the exact impact of air pollution on brain, however, these studies show that the brain is not immune to the ambient air pollution.

Pollution dispersion and diffusion within an urban area is related to the urban aerodynamics. The following sketches show some of the characteristics of such flows and how they generate local areas of accelerating and decelerating winds and vacuum with blowing wind. When wind approaches building structures, there are regions of decreased wind and high pressure, wind separations from the buildings, recirculation areas and large areas of negative pressure and vacuum. Depending on the sources of the pollution and direction of the wind, pollution concentration can be different at different locations within the urban areas. With mobile sources traveling within these areas, the trajectory and concentration of the PM are different, depending on whether it is exposed to the accelerating, decelerating, and recirculating winds or vacuum areas.

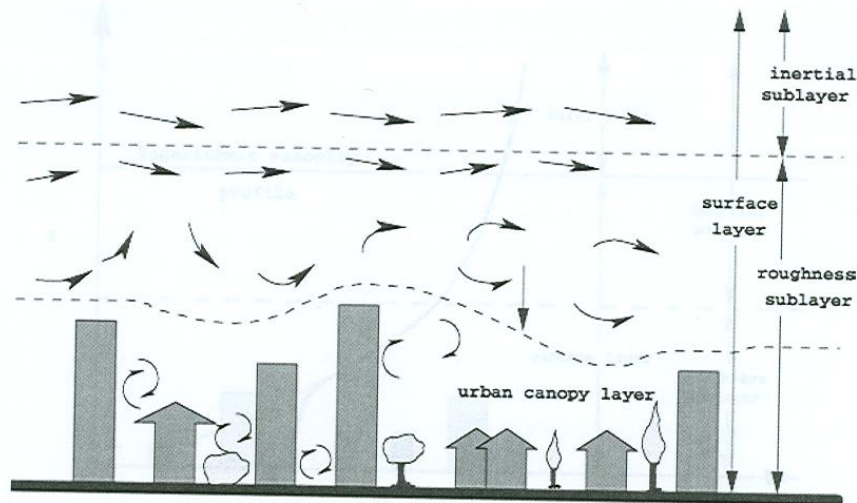


Figure 1. Flow through an urban area [2].

The San Pedro Bay ports of Los Angeles (POLA) and Long Beach (POLB) are among the largest ports in the world. More than 40% of the U.S. containerized trade flows through these ports representing nearly \$300 billion in annual trade. Economic forecasts project this trade to double by the year 2020 [3]. A major adverse impact of this growth is the increase in local and regional air pollution. Diesel engine emissions from the ports activities contribute significantly to the increase in particulate matter (PM),

sulfur oxides (SO_x), and nitrogen oxides (NO_x). Ground level ozone (smog) is formed when NO_x and volatile organic compounds (VOCs) are reacted in the present of sunlight. Reactions of NO_x with ammonia, moisture and other compounds results in nitric acid vapor and related particles which could significantly affect the human respiratory system. NO_x has various derivatives that include nitrous oxide which is a greenhouse gas. Accumulation of greenhouse gases in the atmosphere results in increase in earth's temperature.

Mobile sources such as diesel locomotives and diesel trucks that carry goods from the POLA and POLB, travel through heavily congested areas with massive concentrations of commercial and residential buildings and spaces. These areas are significantly affected by the local concentration of ambient pollution from the port traffics. The objective of the present investigation was to study PM concentration near a building structure from the passage of diesel locomotive. The study is focused on the effect of distortion caused by the building structure on aerosol concentration at different locations upstream of the structure.

BACKGROUND

The rapid distortion theory for a turbulent flow is based on the assumption that the turbulent strain rate is much less than the mean strain rate which requires that the time of distortion is small enough that the viscous dissipation does not produce significant changes in the turbulent kinetic energy. Among the pioneer studies on the effect of non-homogeneous distortions on turbulent velocity field and passive scalars are those by Hunt [4], Wyngaard [5], and Wyngaard et al [6]. These studies have shown that depending on the size of the integral scale of the approaching flow with respect to the dimension of the object, the intensity of the turbulence upstream of the object would be different. When the scale of turbulence is higher than the dimension of the object, the intensity decreases and when it is less, the turbulence intensity increases. The effects of distortion and shear on a passive scalar as shown by Rahai and LaRue [7,8,9] are different, where for different scales of turbulence, the rms scalar remains unchanged within an integral scale upstream of the object and decreases afterward. However, the diffusion of the scalar variance increases and decreases respectively, when the turbulence scale is less than or higher than the object's dimension.

The mean strain rate along the mean stagnation streamline upstream of the object can be estimated as [7]:

$$U^d = U \left(1 - \frac{a^2}{x^2}\right) \quad (1)$$

Here U is the mean velocity, d means distorted, a is object dimension (radius or half-thickness), and x is the axial distance upstream from the center of the object. Taking s as the passive scalar, the effects of distortion on the scalar field is presented as:

$$s^d = s + \frac{U}{c_p} \left(1 + (R - 1) \left(\frac{U^d}{U}\right)^2\right) u \quad (2)$$

Here, *u* is the axial rms turbulent velocity, R is a recovery factor, and *C_p* is the specific heat. The recovery factor is related to temperature difference or heat transfer and for low speed flow with nearly isothermal condition, the recovery factor can be assumed to be zero.

Assuming the diesel PM as a passive scalar, a goal of the investigation was to investigate whether the above relations, especially equation 2, can be used to estimate the concentration of the PM upstream of the building structures within urban areas.

3.0. MEASUREMENT SYSTEMS, PROCEDURE AND TECHNIQUES

3.1 Measurements System

The measurement system components consisted of a TSI condensation particle counter (CPC) model 3772, a TSI DustTrak model 8520, a Setra System pressure transducer model connected to a 0.3175 cm OD pitot static tube, a Young Model 05106 wind monitor-MA, and a Campbell Scientific Wind monitor anemometer model 014A.

The CPC unit operates by drawing aerosol sample continuously through a heated saturator, in which alcohol is vaporized and diffused into the sample stream. The aerosol sample and the alcohol vapor passed into a cooled condenser where the alcohol vapor becomes saturated and ready to condense. Particles present in the sample stream serve as condensation sites for the alcohol. Once condensation begins, particles grow quickly into larger alcohol droplets and pass through an optical detector where they are counted easily. The CPC model 3772 has a range of $0-10^4$ particles/cm³ at $\pm 10\%$ accuracy at an inlet flow rate of 1 ± 0.05 L/min. Higher range is obtainable with larger variations.

The TSI DustTrak uses light scattering technology to determine mass concentration in real-time. A continuous stream draws aerosol sample into a section of a sensing chamber which is illuminated by a small laser beam light. Particles in the aerosol sample scatter light in all directions where some are collected and focused on a photodetector which converts the light into the voltage. The voltage is linearly proportional to the mass concentration of the aerosol. The scattered light depends upon the particle size. The smallest detectable particle for this unit is about $0.1 \mu\text{m}$. The unit is supplied with three different inlet nozzles for different size particle measurements. For the present investigations, the $2.5 \mu\text{m}$ inlet nozzle is used. The time interval for collecting samples was set at either 1 or 5 seconds. The unit was placed in an environmental enclosure with rechargeable battery for continuous unattended sampling. The aerosol sampling inlet is attached to the outside of the enclosure and is connected to unit inside via tubing. The unit can be operated without recharge between 8 hours to one month based on the sampling rate. For our measurements, initially a one second sampling rate was selected, but later the rate was increased to 5 seconds to allow for 24 hours measurement cycle.

For the wind tunnel wind speed measurement, a Setra system pressure transducer model 239 with ± 5 inch water range connected to a small pitot static tube inside the wind tunnel were used. The transducer was connected to a 14 bit National Instrument data acquisition model 6009, connected to a Dell laptop computer. At each pressure measurement location, 1024-4096 samples at a sample rate of 1024 were collected and averaged to estimate the mean velocity.

For the field tests, local wind speed and direction were measured using either a Young model 05106 wind monitor-MA which can measure speed between 0-100 m/sec. and wind direction range of 0-360° for outputs of 0-5 VDC with an overall accuracy of $\pm 1\%$ of the full range or a Campbell Scientific wind monitor system 014A which has a range of 0-100 MPH with an accuracy of 1 MPH.

1.2.Laboratory Measurements

In order to perform the laboratory experiments for investigation of the effects of distortion on the PM concentration, an open circuit wind tunnel adjacent to a diesel engine and in an open laboratory with sufficient air circulations had to be constructed. Figure 2 shows the wind tunnel. The frame for the wind tunnel working area was constructed from 2 inch-squared cross section extruded aluminum bars. The working area cross section is 91.44 cm (36 inch) x 91.44 cm (36 inch) and is 487.68 cm (192 inch) long. A 4 inch thick aluminum honeycomb followed by a screen with 36% solidity placed at the intake of the working area for flow conditioning. A 4:1 contraction connect the working area to a diffuser with an intake cross section of 45.72 cm (18 inch) x 45.72 cm (18 inch). The diffuser is approximately 210 cm (84 inch) long and is connected to a vane axial fan with 76.2 cm (30 inch) diameter and a maximum flow capacity of 13,500 CFM.



Figure 2. The open-circuit wind tunnel

Diesel exhaust from a Vanguard 3-cylinder naturally aspired liquid-cooled diesel engine connected to an electric dynamometer with a maximum output power of 20 BHP at 3600 rpm was used for this part of the investigations. The exhaust was introduced perpendicular to the flow inside the wind tunnel via a 5.08 cm (2 inch) ID high temperature flexible tube connected to a 5.08 cm (2 inch) ID , and 30.48 cm (12 inch) long aluminum tube (Figure 3). The tube was protruded through the bottom section of the wind tunnel by 5.08 cm (2 inches) at 76.2 cm (30 inches) from the entrance of the wind tunnel working area. The diesel exhaust volume flow rate was approximately 0.6 m³/min, which corresponds to an approximate mean velocity of 14.84 m/sec.



Figure 3. Diesel exhaust.

A cylindrical tube of 8.89 cm (3.5 inch) diameter, d , and 76.2 cm (30 inch) in length and a rectangular block of 7.62 cm (3 inch) squared cross section (t^2) with the same length as the cylinder tube were used as the distorting objects (Figure 4). The objects were placed individually at mid-section at 60 cm from the exit of the working area. The blockage was less than 8%. Results were not corrected for the blockage effect.

The experiments were performed at wind speeds of approximately 2.7 (1.24 m/sec.), 5.8 (2.63 m/sec.), and 8.2 (3.72 m/sec.) miles per hour (MPH) and constant diesel exhaust.



Figure 4. The distorting objects.

1.3. Field Tests

Field tests were performed adjacent to the Alameda Corridor railroad at the Commodore Heim Bridge, at the intersection of the Henry Ford and Anchorage roads. The field tests were performed under the bridge adjacent to the control room at locations where distortion due to the building structure was present (Figure 5). Measurements of PM and wind speeds were made continuously over several days and data was correlated with the passage of diesel trains.



Figure 5. Field test measurements.

4.0. RESULTS AND DISCUSSION

4.1. Laboratory Results

Variation of the free stream mean velocity and PM concentration are measured upstream of the object at x/D (or x/t) = 6 where the effects of distortions were not present. Figures 6 and 7 show results of these experimentations. For each configuration, the engine was run for a warm up period and exhaust measurement was performed to ensure stable condition, before conducting the experiment. Here Y/D (or Y/t) is the vertical distance with zero indicates the mid-section of the wind tunnel. Single set of measurements were performed for each case. For the cylinder, variation in the mean velocity is increased with increasing the mean velocity, however the maximum variation is less than 10%. These variations are related to the inlet flow conditions as there was no settling chamber and contraction for improving the uniformity of the flow.

Variation in the PM concentration is related to the ratio of the exhaust jet and free stream mean velocity. For large ratio (low free stream velocity), the PM concentration increases at high vertical distances while with reduced ratio (increased free stream velocity), the high concentration of the PM is moved toward the wind tunnel bottom surface. These conditions are observed for measurement of PM concentration upstream of the objects at different free stream mean velocities. Similar characteristics are found for the rectangular object with slight variations.

As stated in the background, the major parameter that affects the concentration of a passive scalar is the ratio of the integral length scale to the typical dimension of the object. For the present experiment, the estimated ratio is higher than or equal to the dimensions of the objects and thus, discussions as related to the effect of distortion on PM variation are presented with respect to these conditions.

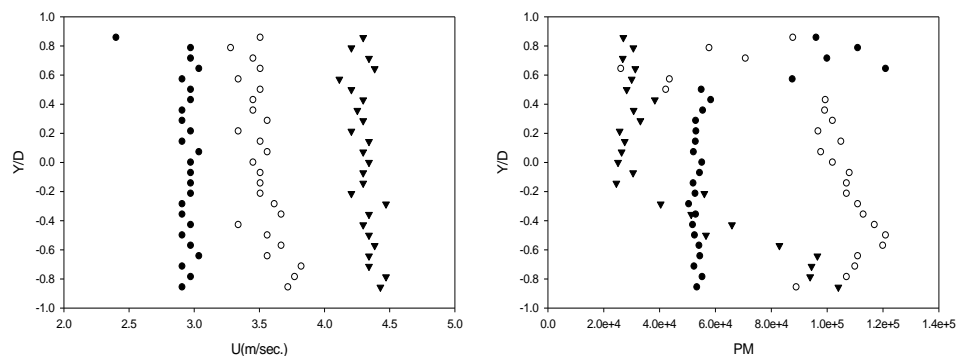


Figure 6. Variation of the free stream mean velocity and PM concentration ($\#/cm^3$) for the cylinder. Open circle, solid circle, and solid triangle are at 2.7, 5.8, and 8.2 miles/hr respectively.

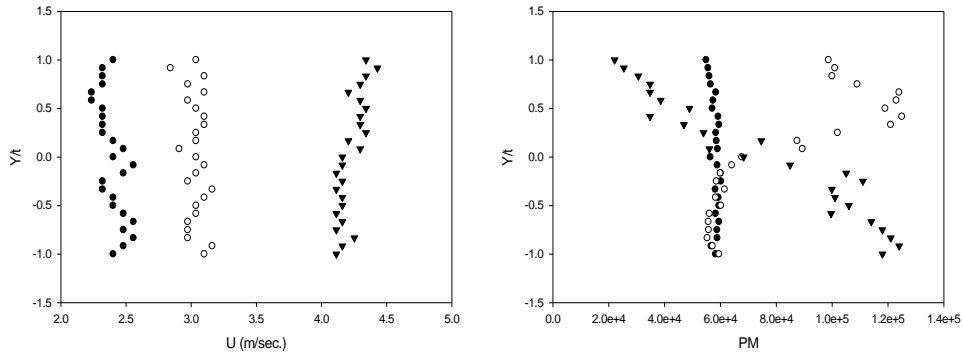
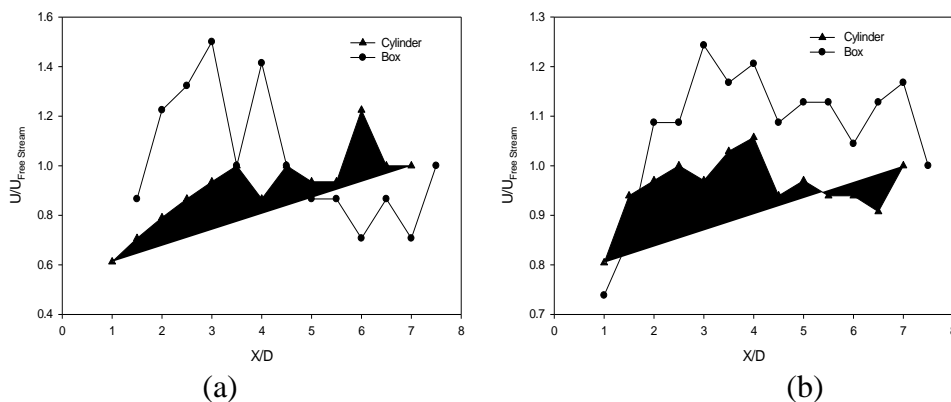


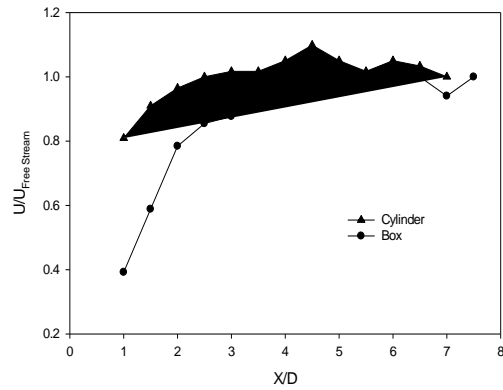
Figure 7. Variation of the free stream mean velocity and PM concentration ($\#/cm^3$) for the rectangular object. Symbols the same as Figure 6.

Figures 8 and 9 show variation of the normalized mean velocity and PM concentration along the mean stagnation streamlines upstream of the objects at (a) 2.7 MPH, (b) 5.8 MPH, and (c) 8.2 MPH. The mean velocity is reduced near the object and the decrease in mean velocity extends to further upstream location with increasing the free stream velocity. These effects are more pronounced for the rectangular object.

At 2.7 MPH, the normalized PM is near one, up to $x/D = 4.5$ where it starts to fluctuate and then increases as it approaches the objects. With increase in the free stream mean velocity, the increase in PM extends further upstream and at 8.2 MPH it increases to more than 20% for the rectangular object while the increase is not significant for the cylindrical object.

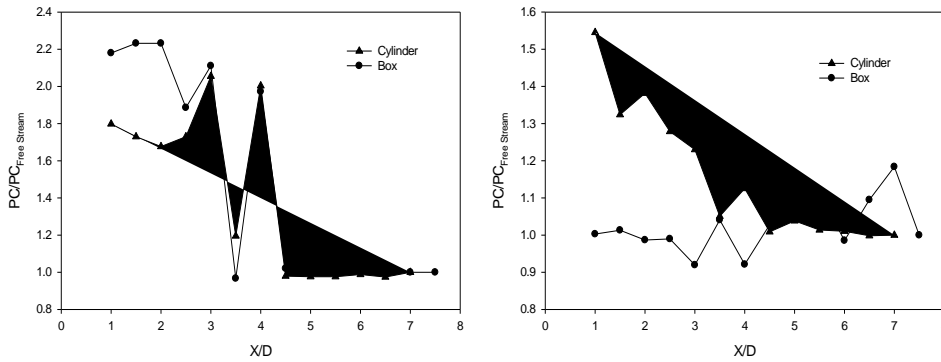
Variation of the PM shows that the blockage plays a major role in the local concentration of the PM. With the rectangular object, the stagnant flow area is large and thus larger blockage effect and higher level of PM concentration. However, for the cylinder the blockage is much less and thus the increase in the PM concentration near the object is not as significant.





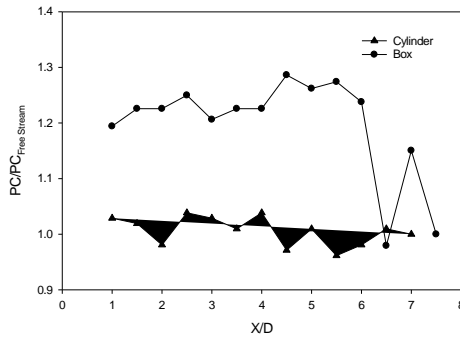
(c)

Figure 8. Variation of the normalized mean velocity along the mean stagnation streamlines for (a) 2.7 MPH, (b) 5.8MPH, and (c) 8.2 MPH.



(a)

(b)



(c)

Figure 9. Variation of normalized PM at free stream velocity of (a) 2.7 MPH, (b) 5.8 MPH, (c) 8.2 MPH.

Figure 10 shows normalized scalar concentration, obtained from equation 2 according to the mean velocity data and PM concentration from the present experiments for the rectangular object. Similar results are obtained for the cylindrical object. As it could be seen, there is no variation in the scalar concentration with respect to upstream distance and changes in the mean velocity. Since the recovery factor is nearly zero, the

contributions to the normalized distorted scalar come from the local mean and turbulent velocities and the specific heat at constant pressure. Since the specific heat which is in the denominator is several order of magnitude larger than the velocity components, then the right hand side of the equation approaches 1, resulting in negligible variation in the distorted concentration. Thus, within the urban environment, equation 2 is not an appropriate model to predict the local PM concentration at different locations.

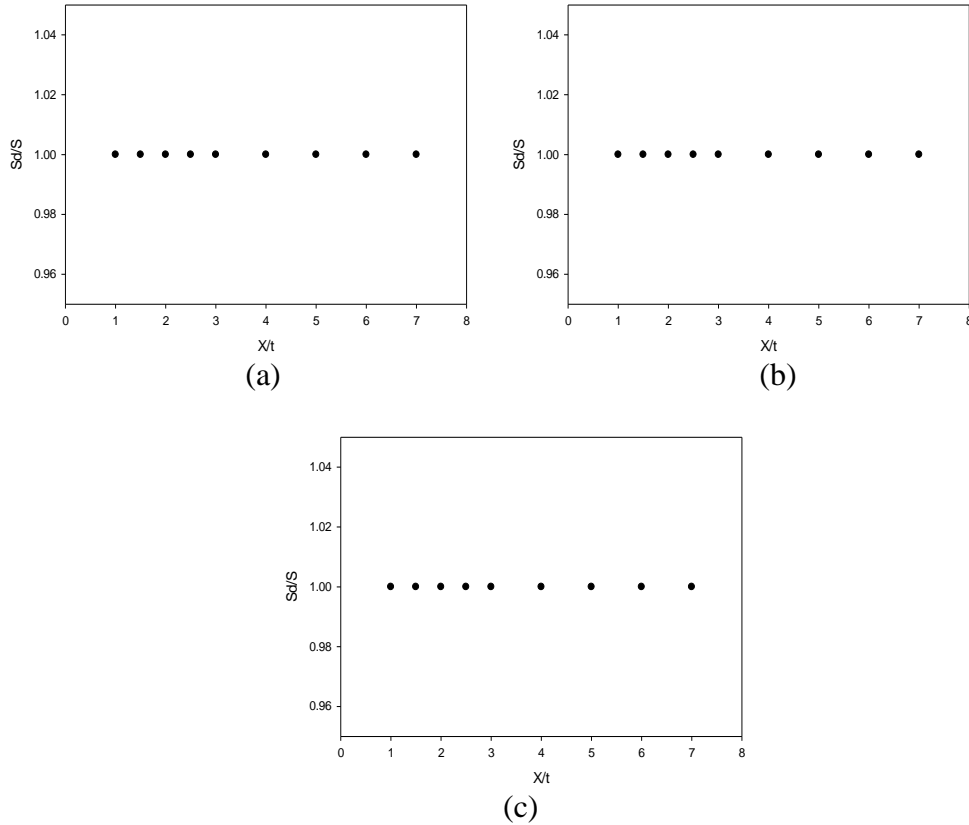


Figure 10. Variation of normalized scalar from equation 2 at free stream velocity of (a) 2.7 MPH, (b) 5.8 MPH, (c) 8.2 MPH.

Considering the present laboratory results where the PM concentration increases with the mean velocity, another possible model could be the following equation:

$$\alpha = \alpha_0 + Ae^{-Bx} \quad (3)$$

Here $\alpha = \frac{PM_d}{\frac{PM}{U_d}}$, the ratio of the normalized PM to the normalized velocity, α_0 is the corresponding value at $x=0$, and A and B are constants to be determined. Figure 11 shows variations of α with the upstream distances. From fitting the equation 3 to the average values at each location, the constants are: $\alpha_0=1.04$, $A=2.38$, and $B=-0.8$. The correlation coefficient is 0.975.

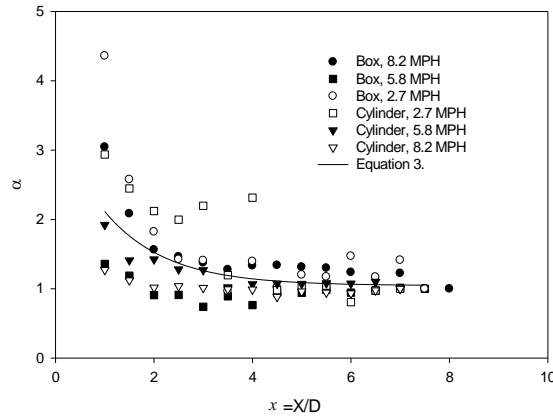


Figure 11. Variation of the ratio of normalized PM to normalized velocity with upstream distance.

Equation 3 with the corresponding coefficients impose a maximum value of 3.42 for α at $x = 0$ which might not be correct, especially at low wind speeds. Further measurements are required for development of a more accurate model for prediction of the PM concentration with respect to the variation of the mean velocity and the local blockage effect.

4.2. Field Measurements

Figures 12 and 13 show temporal variations of the PM, wind speed and direction for two locations of near the wall and at a distance equivalent to the height (h) of the control room structure. Here the wind direction is measured from north (zero degree), increasing in counter clockwise direction. There are significant variations in PM concentration at $x=h$ which corresponds to the variations in the wind speed. The wind direction was mostly at either around 100 degrees (SE) or 300 degrees (NW). Since the wind direction was not perpendicular to the structure, the level of variation in PM concentration could be due to wind-structure interaction with NW wind moving toward the structure at slanted angle and SE wind moving away from the structure. Occasional south and north direction wind also has contributed to these variations.

Near the wall, the concentration of PM is nearly constant, except when there are increases in the wind speed. The direction of the wind is mostly NW (toward the structure) which explains reduced variation in PM concentration.

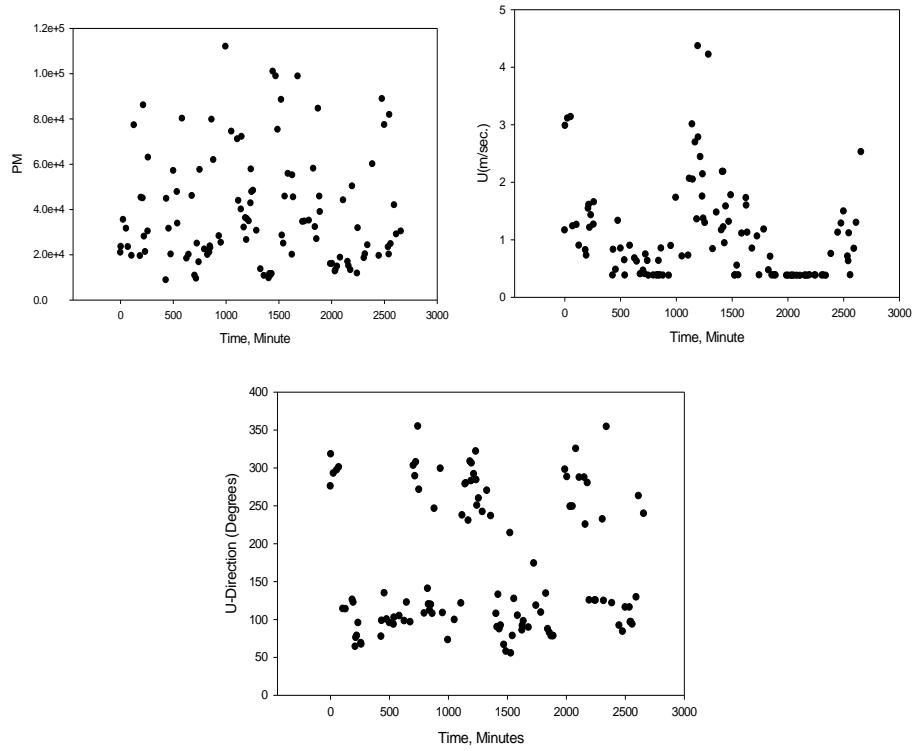


Figure 12. Temporal variation of PM, wind speed and direction from the field test measurements at $x=h$.

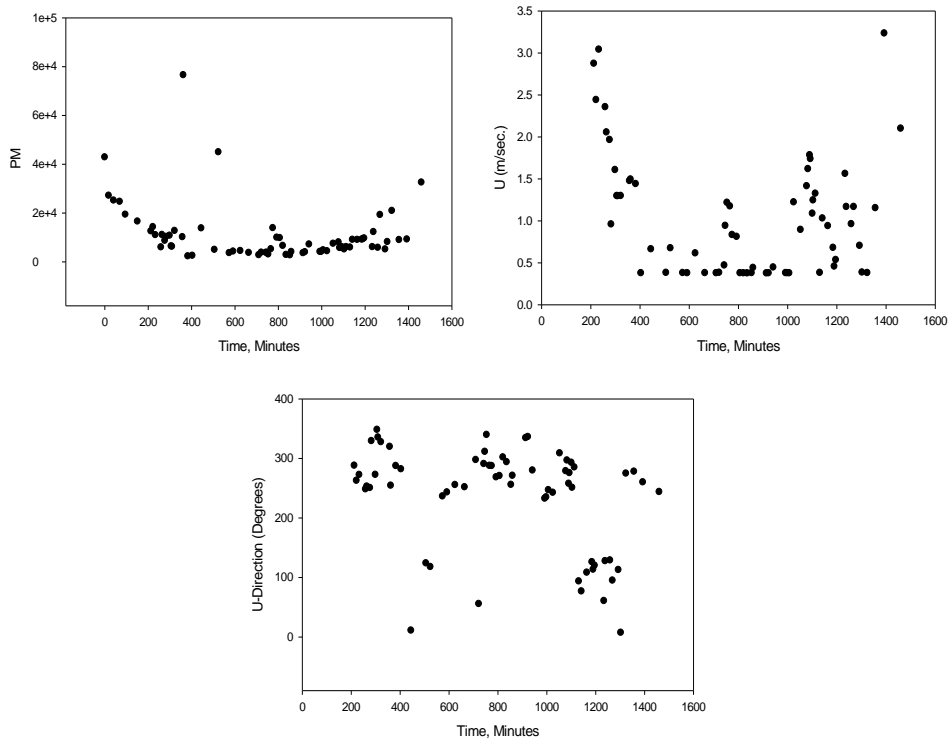


Figure 13. Temporal variation of PM, wind speed and direction from the field test measurements near the wall.

5.0. CONCLUSIONS AND RECOMMENDATIONS

The effects of distortion caused by blockages and structure on trajectory of diesel particulate matter (PM) have been investigated. The investigation was divided into two parts. In part one, laboratory investigations were performed using an open circuit low speed wind tunnel and diesel exhaust from a 3-cylinder diesel engine. The experiments were performed at wind speeds of approximately 2.7 (1.2 m/sec.), 5.8 (2.6 m/sec.), and 8.6 (3.9 m/sec.) miles per hour and diesel exhaust was injected perpendicular to the flow at approximately 60 cm from the working area entrance at the mid-section. The diesel exhaust volume flow rate was approximately $0.6 \text{ m}^3/\text{min}$, which corresponds to a mean velocity of 14.8 m/sec.

A cylindrical tube of 8.89 cm (3.5 inch) diameter, d , and 76.2 cm (30 inch) in length and a rectangular block of 7.62 cm (3 inch) squared cross section (t^2) with the same length as the cylinder tube were used as the distorting objects. The wind tunnel cross section was 91.4 cm x 91.44 cm (36 inch x 36 inch) and 4.8 m long. The objects were placed individually at the mid-section at 60 cm from the exit of the working area. The blockage was less than 8%. Results were not corrected for the blockage effect.

Measurements of the wind velocity and aerosol concentration were made upstream of the object, using a 0.3175 cm diameter pitot tube and a TSI condensation particle counter model 3772. Measurements were carried out along the stagnation streamline up to 8d (or 8t) upstream of the objects. Increasing PM concentrations are observed at all speeds as the objects are observed.

Part two of the investigation was focused on field tests under actual environmental conditions. Field tests were performed adjacent to the Alameda Corridor railroad at the Commodore Heim Bridge, at the intersection of the Henry Ford and Anchorage roads. The field tests were performed under the bridge adjacent to the control room at the location where distortion due to the building structure was present. Measurements of the PM and the wind speeds were made continuously over several days and data was correlated with the passage of diesel trains. Results were in agreement with the experimental results when the local wind shear characteristics were taken into consideration.

Overall, the diesel PM concentration is significantly affected by the wind velocity and the blockage imposed by the structure. When wind is blowing toward the structure, with high blockage effect, there are significant increases in the PM concentration near the wall with relatively constant distribution. However, the level is significantly reduced if the blockage effect is not significant. These results indicate that the PM concentration within urban areas has strong correlation with local urban aerodynamics.

REFERENCES

1. Campbell, A., Oldham, M., Becaria, A., Bondy, S.C., Meacher, D., Sioutas, C., Misra, C., Mendez, L.B., and Kleinman, M., 2005, "Particulate Matter in Polluted Air May Increase Biomarker of Inflammation in Mouse Brain", *Neurotoxicology*, 26(1): 133-140.
2. Britter, S., and Hanna, S., 2003, "Flow and Dispersion in Urban Areas," *Annu. Rev. Fluid Mech.* 35, 469-96.
3. Port of Los Angeles Inventory of Air Emissions, 2005. ADP#050520-525
4. Hunt, J.C.R., 1973, "A Theory of Two-dimensional Flow Round Two-dimensional Bluff Objects," *J. Fluid Mech.*, 61, 625.
5. Wyngarrd, J.C., 1981, "The Effects of Probe-Induced Flow Distortion on Atmospheric Turbulence Measurements," *J. Appl. Meteorol.*, 20, 784-794.
6. Wyngaard, J.C., Rockwell, L., and Friehe, C., 1985, "Error in the Measurements of Turbulence Upstream of an Axi-symmetric Body," *J. Atmos. Ocean Tech.*, 2, 605-614.
7. Rahai, H.R., and LaRue, J.C., "Decay of Temperature variance in the Presence of Non-homogeneous Strain," *ASME Journal of Fluids Engineering*, Vol. 14, No. 2., 1992.
8. Rahai, H.R. and LaRue, J.C., "Distortion of a Turbulent Scalar Upstream of Axisymmetric Objects," *AIAA J. of Thermophysics and Heat Transfer*, Vol.7, No.3, 1993.
9. Rahai, H.R., and LaRue, J., 1995, "The Distortion of a Passive Scalar by Two-Dimensional Objects," *Physics of Fluids*, 7(1), pp 98-107.
10. Rahai, H., "Development of an Exposure Model for Diesel Locomotive Emissions Near the Alameda Corridor," Final Report, METRANS contract no. AR-05-03, Feb. 21, 2008.